Maurocalcine interacts with the cardiac ryanodine receptor without inducing channel modification

Xavier ALTAFAJ*, Julien FRANCE*, Janos ALMASSY†, Istvan JONA†, Daniela ROSSI‡, Vincenzo SORRENTINO‡, Kamel MABROUK§, Michel DE WAARD* and Michel RONJAT*[1]

*iRTSV/CCFP CEA Grenoble INSERM U836 Institut des Neurosciences Grenoble GIN, 17 rue des Martyrs, 38054 Grenoble Cedex 09, France, †Department of Physiology, Research Center of Molecular Medicine, Medical and Health Science Center, University of Debrecen, Debrecen, Hungary, ‡Molecular Medicine Section, Department of Neuroscience, University of Siena, Siena, Italy, and §Universités D'Aix-Marseille 1, 2 et 3 CNRS-UMR 6517, Chimie, Biologie et Radicaux libres, Case 521Av.Esc. Normandie Niemen 13397 Marseille Cédex 20, France

We have previously shown that MCa (maurocalcine), a toxin from the venom of the scorpion *Maurus palmatus*, binds to RyR1 (type 1 ryanodine receptor) and induces strong modifications of its gating behaviour. In the present study, we investigated the ability of MCa to bind to and modify the gating process of cardiac RyR2. By performing pull-down experiments we show that MCa interacts directly with RyR2 with an apparent affinity of 150 nM. By expressing different domains of RyR2 *in vitro*, we show that MCa binds to two domains of RyR2, which are homologous with those previously identified on RyR1. The effect of MCa binding to RyR2 was then evaluated by three different approaches: (i) [^{3}H]ryanodine binding experiments, showing a very weak effect of MCa (up to 1 μM), (ii) Ca^{2+} release measurements from cardiac sarcoplasmic reticulum vesicles, showing that MCa up to 1 μM is unable to induce Ca^{2+} release, and (iii) single-channel recordings, showing that MCa has no effect on the open probability or on the RyR2 channel conductance level. Long-lasting opening events of RyR2 were observed in the presence of MCa only when the ionic current direction was opposite to the physiological direction, i.e. from the cytoplasmic face of RyR2 to its luminal face. Therefore, despite the conserved MCa binding ability of RyR1 and RyR2, functional studies show that, in contrast with what is observed with RyR1, MCa does not affect the gating properties of RyR2. These results highlight a different role of the MCa-binding domains in the gating process of RyR1 and RyR2.

Key words: calcium channel, excitation–contraction coupling, heart, maurocalcine, ryanodine receptor, toxin.

INTRODUCTION

Ca^{2+} signalling is a crucial step in the regulation of major cellular functions. Oscillations of cytosolic Ca^{2+} concentration result from the balance between mechanisms allowing cytoplasmic Ca^{2+} increase (influx from extracellular medium and release from intracellular stores) and their counterparts allowing Ca^{2+} storage in the ER (endoplasmic reticulum) and Ca^{2+} efflux. Ca^{2+} release from the ER is due to the activation of two different families of intracellular Ca^{2+} channels, the RyRs (ryanodine receptors) and the IP3Rs (inositol trisphosphate receptors). The RyR family is composed of three protein isoforms encoded by three different genes: the RyR1 or skeletal muscle isoform, the RyR2 or cardiac muscle isoform and the RyR3 isoform, which show a ubiquitous expression pattern [1]. Although the three isoforms exhibit a relatively conserved amino acid sequence and an overall similar regulation by the cytoplasmic Ca^{2+} concentration and various effectors, different mechanisms have been proposed to control their activation following plasma membrane depolarization. Indeed, while physiological RyR2 activation requires Ca^{2+} influx through the cardiac DHPR (dihydropyridine receptor), according to the mechanism of CICR (Ca^{2+}-induced Ca^{2+} release), RyR1 has been proposed to be conformationally coupled to the DHPR skeletal isoform and to be activated in response to charge movements within the DHPR following plasma membrane depolarization. The molecular basis of these processes has been investigated by studying the coupling between the DHPR and RyR when expressing different pairs of isoforms. Expression of a cardiac DHPR $Ca_v1.2$ subunit in skeletal muscle cells of dysgenic mice ($Ca_v1.1^{-/-}$) as well as expression of RyR2 in skeletal muscle cells lacking RyR1 results in the CICR process [2,3]. These results clearly indicate that the differences in RyR physiological regulation processes rely not only on the DHPR moiety, but also on intrinsic gating properties specific to each RyR isoform.

Toxins issued from spider, snake or scorpion venoms are strong effectors of ion channels, converting these peptides into very valuable tools for the study of channel properties. In the last decade five scorpion toxins, IpTxA (imperatoxin A), MCa (maurocalcine), BjTx-1/2 (*Buthodus judaicus* toxins 1 and 2) and hemicalcin have been shown, *in vitro*, to activate RyR1 [4–7]. Although all of them promote an increase of [^{3}H]ryanodine binding on RyR1 and induce RyR1 opening at subconductance states, MCa appears to be the strongest effector of RyR1 in terms of affinity, increase of ryanodine binding and duration of the induced subconductance opening events.

Using a site-directed mutagenesis approach, we previously identified a stretch of basic amino acid residues critical for MCa effects on RyR1 [8]. Interestingly this domain shows some sequence similarities with a discrete region (domain A) of the cytoplasmic II-III loop of the DHPR $Ca_v1.1$ subunit, the physiological activator of RyR1 in skeletal muscle [9]. Based on this similarity, MCa and IpTxA have been used to study the functional role of the DHPR domain A [10,11]. In skeletal muscle cells, these toxins have been shown to increase the frequency and to modify the characteristics of RyR1-mediated Ca^{2+} release events [12,13].

We recently identified two discrete domains of RyR1 responsible for its interaction with MCa [14]. We showed that these two

Abbreviations used: CICR, Ca^{2+}-induced Ca^{2+} release; DHPR, dihydropyridine receptor; ER, endoplasmic reticulum; HSR, heavy sarcoplasmic reticulum; IpTxA, imperatoxin A; LLSS, long-lasting subconductance state; MCa, maurocalcine; RyR, ryanodine receptor; SR, sarcoplasmic reticulum.

[1] To whom correspondence should be addressed (email mronjat@cea.fr).

domains also bind a synthetic peptide corresponding to domain A of the DHPR. These results strengthened the hypothesis that MCa mimics the effect of domain A on RyR1. The fact that these amino acid sequences are relatively conserved between RyR1 and RyR2 prompted us to evaluate the binding and functional effect of MCa on RyR2.

In the present study, we demonstrate that MCa physically interacts with the purified RyR2 isoform. This interaction takes place within amino acid regions of RyR2 homologous with the previously identified MCa-binding domains of RyR1. However, in sharp contrast with what is observed on RyR1, we show that MCa has a negligible effect on [^{3}H]ryanodine binding on RyR2, fails to induce Ca^{2+} release from cardiac SR (sarcoplasmic reticulum) vesicles and does not modify gating properties of purified RyR2 incorporated into a planar lipid bilayer. These results highlight a different involvement of the MCa-binding domains in the control of the gating process of RyR1 and RyR2.

EXPERIMENTAL

Cloning and expression of RyR1 and RyR2 fragments

cDNAs encoding fragments F3 and F7 of RyR1 (corresponding to amino acids 1022–1631 and 3201–3661 respectively) and fragments F3 and F7 of RyR2 (corresponding to amino acids1033–1622 and 3158–3609 respectively) were cloned by a PCR-based approach using full length cDNAs as a template (GenBank® accession number for RyR1 and RyR2 are X15750 and M59743 respectively). The RyR1 F3 and F7 fragments were cloned as described previously [14].

The RyR2 F3 fragment was cloned using the following primers: forward 5′-GTTCCTTACACTCTTCTAGAT-3′ and reverse 5′-CAAACACTGCACCAGCCAGCC-3′. A Kozak consensus sequence (GCCGCCACC) was added before the ATG start codon and the amplified F3 fragment was cloned in between the EcoRV and BamHI sites of the pcDNA3.1/myc vector (Invitrogen).

The RyR2 F7 fragment was cloned using the following primers: forward 5′-GTTTGTCTTGCTGCTTTTGCTG-3′ and reverse 5′-ATATAAGGGAGCCATTCGGAA-3′. A Kozak consensus sequence (GCCGCCACC) was added before the ATG start codon and the amplified F7 fragment was cloned in between the EcoRV and HindIII sites of the pcDNA3.1/myc vector (Invitrogen).

RyR fragments were then expressed using a coupled *in vitro* transcription and translation system (TrT® kit, Promega), according to the manufacturer's instructions, allowing the expression of ^{35}S-labelled RyR1 or RyR2 F3 and F7 fragments.

HSR (heavy SR) vesicle preparation

HSR vesicles from rabbit skeletal muscle were prepared as described in [15]. Cardiac HSR vesicles where prepared from canine heart left ventricle muscle as described in [16]. The protein concentration was measured using the Bradford method [16a].

RyR purification

RyR1 and RyR2 were purified from CHAPS-solubilized skeletal and cardiac muscle HSR vesicles using the sucrose gradient technique [16,17].

Pull-down experiments

Streptavidin-coated polystyrene magnetic beads (500 μg, Dynal) were incubated for 30 min at room temperature (20 °C) in PBS (pH 7.4) in the presence of biotinylated MCa (40 μM final concentration) or biotin (control) and then washed three times with PBS. MCa- (or biotin-) coated beads where incubated with purified RyR1, purified RyR2 or [^{35}S]RyR2 fragments, for 2 h at room temperature in buffer A [150 mM NaCl, 20 mM Hepes, pH 7.4, 2 mM EGTA and 2 mM $CaCl_2$ (pCa5)] supplemented with protease inhibitors (Complete Mini, Roche) and 0.1 mg/ml BSA. For the measurement of the apparent MCa-binding affinity on RyR2, streptavidin beads were coated with different amounts of biotin–MCa (corresponding to the indicated concentrations) and then incubated with RyR2 in buffer A in the presence of 10 nM [^{3}H]ryanodine. After washing three times with PBS, bound proteins were eluted and analyzed by Western blotting (for RyR1 and RyR2 pull-down experiments), autoradiography (for pull-down of ^{35}S-labelled RyR fragments) after separation by SDS/PAGE or liquid scintillation counting (for pull-down [^{3}H]ryanodine labelled RyR2). RyRs were identified using polyclonal antibodies recognizing the different RyR isoforms [15]. The results are presented as means ± S.E.M. for at least three experiments.

[^{3}H]Ryanodine binding assay

HSR vesicles (cardiac or skeletal; 1 mg/ml) were incubated at 37°C for 2.5 h in buffer A in the presence of 5 nM [^{3}H]ryanodine. MCa was added to the assay buffer just prior to the addition of HSR vesicles. After incubation, HSR vesicles were filtrated through Whatmann GF/B glass filters and washed three times with 5 ml of ice-cold washing buffer (150 mM NaCl and 20 mM Hepes, pH 7.4). [^{3}H]Ryanodine bound to filters was then measured by liquid scintillation counting. Non-specific binding was measured in the presence of 20 μM unlabelled ryanodine. Each experiment was performed in triplicate and repeated at least twice. The results are presented as the means ± S.E.M.

For pull-down experiments, purified RyR2 was labelled with [^{3}H]ryanodine as follows. Purified RyR2 (30 μg/ml) was incubated for 90 min at room temperature in a buffer containing, 150 mM NaCl, 20 mM Hepes, pH 7.4, 10 nM [^{3}H]ryanodine, a cocktail of protease inhibitors and various concentrations of MCa-coated beads. For total binding (B_{max}) measurements, RyR2 was filtrated, after incubation with [^{3}H]ryanodine, on Whatmann GF/B glass filters and washed three times with 5 ml of ice-cold washing buffer. [^{3}H]Ryanodine binding was then measured by liquid scintillation counting. Non-specific binding was measured in similar conditions in the presence of 20 μM unlabelled ryanodine.

RyR2 Ca^{2+}-channel reconstitution and single-channel recording analysis

Channel activity measurements were carried out using purified RyR2 incorporated into a planar lipid bilayer. The bilayer was formed using phosphatidylethanolamine, phosphatidylserine, and L-phosphatidylcholine in a ratio of 5:4:1 (by vol.) dissolved in *n*-decane up to the final lipid concentration of 20 mg/ml. A bilayer was formed across a 200- or 250-μm diameter aperture of a Delrin cap using a symmetrical buffer solution (250 mM KCl, 100 μM EGTA, 150 μM $CaCl_2$ and 20 mM Pipes, pH 7.2). A small aliquot of purified RyR2 was added into one chamber. After successful incorporation we tested the effect of Ca^{2+} on both sides in order to determine the orientation of the incorporated channel. The cytoplasmic and luminal sides were defined as the *cis* and *trans* sides respectively. For the determination of the gating properties of the channel, the Ca^{2+} concentration was adjusted to 472 nM on the *cis* side by addition of EGTA. Electrical signals were filtered at 1 kHz through an 8-pole low-pass Bessel filter and digitized at 3 kHz using Axopatch 200 and pCLAMP 6.03 (Axon Instruments, Union City, CA, U.S.A.).

Ca^{2+}-release measurements

Ca^{2+} release from skeletal or cardiac HSR vesicles was measured using the Ca^{2+}-sensitive dye Antipyrylazo III. The absorbance was monitored at 710 nm by a diode array spectrophotometer (MOS-200 Optical System, Bio-Logic, Claix, France). Vesicles (50 μg) were actively loaded with Ca^{2+} at 37°C in 2 ml of a buffer containing 100 mM KCl, 7.5 mM sodium pyrophosphate and 20 mM Mops (pH 7.0), supplemented with 250 μM Antipyrylazo III and 1 mM ATP/$MgCl_2$. Ca^{2+} loading was initiated by sequential additions of 20 μM (final concentration) of $CaCl_2$. At the end of each experiment, the Ca^{2+} remaining in the vesicles was determined by the addition of Ca^{2+} ionophore A23187 (4 μM) and the absorbance signal was calibrated by two consecutive additions of 20 μM $CaCl_2$. Total recording time in each experiment was 10–20 min for each experimental condition tested. In these conditions, no spontaneous Ca^{2+} release was observed.

RESULTS

MCa interacts with purified RyR2

The interaction of MCa with RyR2 was investigated using a synthetic MCa with a biotinylated lysine residue at the N-terminus, immobilized on streptavidin-coated beads as described previously [14]. Using these MCa-coated beads, we performed pull-down experiments with a purified RyR1 and RyR2 preparation. Figure 1(A) shows that both isoforms of RyR (RyR1 in lane 1 and RyR2 in lane 4) interacted with the MCa-coated beads (lanes 3 and 6), whereas they were not detected on biotin-coated beads (lanes 2 and 5). In order to quantify the interaction of MCa with RyR2, pull-down experiments were done with purified RyR2, in the presence of [^{3}H]ryanodine. The amount of RyR2–MCa complex was then assessed by measuring the [^{3}H]ryanodine bound on to the MCa-coated beads. The results presented in Figure 1(B) show the amount of [^{3}H]ryanodine-labelled RyR2 pulled-down as a function of MCa bead concentration. The B_{max} corresponds to the amount of [^{3}H]ryanodine bound to RyR2, measured under the same conditions by filtration and was 121 $\pm$ 15 pmol/mg. In the presence of 500 nM MCa, approx. 90 % of the RyR is bound to MCa. These results highlight the presence of two populations of RyR within our preparation. The first one represents approx. 10 % of the pulled-down RyR and shows an apparent affinity for MCa of 10 nM, similar to the apparent affinity measured previously for the MCa–RyR1 interaction. The second population represents the large majority of the pulled-down RyR2 population and shows an apparent affinity for MCa of 150 nM. Although these two populations could represent two different states of the RyR2, they could also result from a slight contamination of the preparation with RyR1. In this case, one has to consider that since MCa induces an 8–10-fold increase of [^{3}H]ryanodine binding on RyR1, this contamination would, in fact, represent only 1 % of the total RyR2 population. In both cases, these results show that MCa interacts with RyR2, although with an apparent affinity lower than with RyR1. It is important to note that interaction experiments of MCa with [^{3}H]ryanodine-labelled RyR2 take into account only the tetrameric RyR2 (the only form able to bind ryanodine). This is likely to explain the apparent higher yield of the pull-down of [^{3}H]ryanodine-labelled RyR2 compared with the yield of the pull-down measured by Western blot that takes into account the total RyR2 population.

To characterize further the RyR2 domains that interact with MCa, we aligned the sequences of previously identified RyR1 MCa-binding domains (namely the F3 and F7 domains [14]), with equivalent RyR2 sequences, using the ClustalW

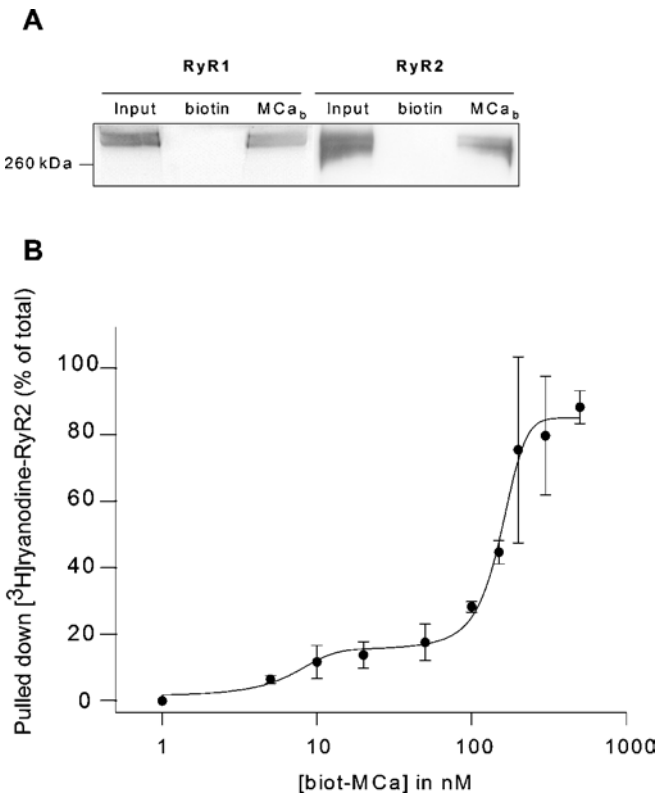

Figure 1 MCa interacts with RyR2

(**A**) Western blot analysis of pull-down experiments showing a direct interaction of MCa with purified RyR1 and RyR2. Purified RyR1 and RyR2 were obtained as described in the Experimental section. Streptavidin-coated magnetic beads covered with either biotin or biotinylated MCa (MCa$_b$) were incubated with purified RyR1 or RyR2 and the bound proteins analysed as described in the Experimental section. (**B**) Concentration-dependence relationship of the MCa–RyR2 interaction. Purified RyR2 was incubated with an increasing concentration of biotin–MCa coated on streptavidin beads in the presence of 10 nM [^{3}H]ryanodine for 90 min at room temperature. Beads were then washed and [^{3}H]ryanodine bound on MCa-coated beads was measured by liquid scintillation counting. Non-specific binding was measured in the presence of 20 μM unlabelled ryanodine. The total amount of [^{3}H]ryanodine–RyR complex (B_{max}) was measured in identical conditions using a filtration technique.

software [18] (http://www.ebi.ac.uk/clustalw). This comparison shows that fragments F3 and F7 share 54.2 % and 63.2 % amino acid identity with the corresponding fragments of RyR2. Based on this alignment, RyR2 F3 and F7 domains encompassing amino acids 1033–1622 and 3158–3609 respectively, were cloned and expressed *in vitro* as ^{35}S-radiolabelled proteins. The interaction of these fragments with MCa was then measured by pull-down experiments as described above. The results presented in Figure 2(A) show that, similarly to RyR1 F3 and F7 domains, the F3 and F7 domains of RyR2 interacted specifically with MCa. Quantitative analysis (Figure 2B) shows that approx. 15 % of RyR2 F3 and approx. 50 % of RyR2 F7 fragments were bound to MCa-coated beads.

Effect of MCa on [^{3}H]ryanodine binding on RyR2

As described previously, MCa is one of the most powerful effectors of RyR1 [8]. This effect of MCa has been associated to its interaction with discrete domains of RyR1 and deletion of the F7 domain leads to a RyR1 channel that is insensitive to MCa [14]. Since MCa interacts with homologous F3 and F7 fragments of RyR2, we evaluated the ability of MCa to modify RyR2 properties. We first studied the effect of MCa on [^{3}H]ryanodine binding

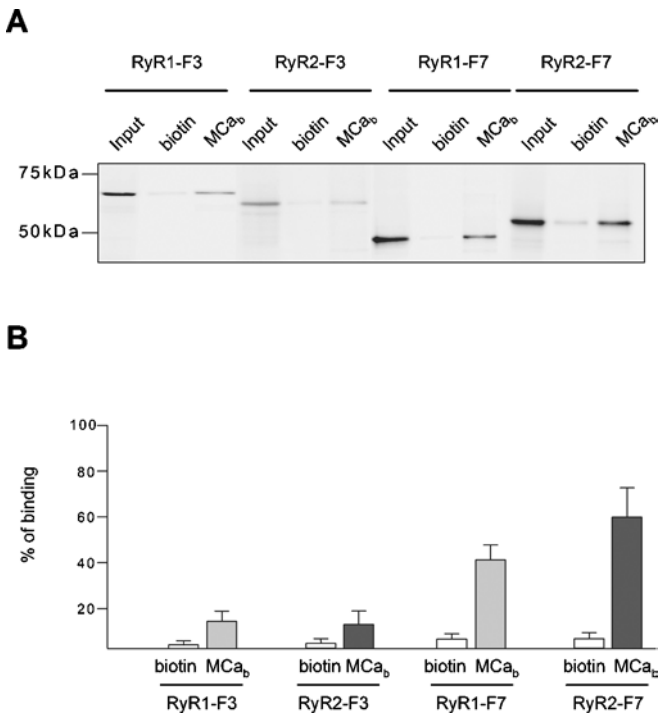

Figure 2 MCa interacts with discrete domains (F3 and F7) of RyR1 and RyR2

(**A**) RyR1 F3 and F7 domains and the corresponding domains of RyR2 were expressed *in vitro* as radiolabelled proteins (input lanes), as described in the Experimental section. Each fragment was then incubated in the presence of polystyrene magnetic beads coated either with biotin or biotinylated MCa (MCa_b). The interaction of each fragment with MCa-coated beads was measured by autoradiography after separation by SDS/PAGE. (**B**) Statistical analysis of the interaction of *in vitro* translated F3 and F7 fragments of RyR with biotin (open bars) or MCa_b (grey bars for RyR1 fragments and closed bars for RyR2 fragments). Binding was estimated by densitometric analysis and expressed as the means ± S.E.M. for at least three independent experiments.

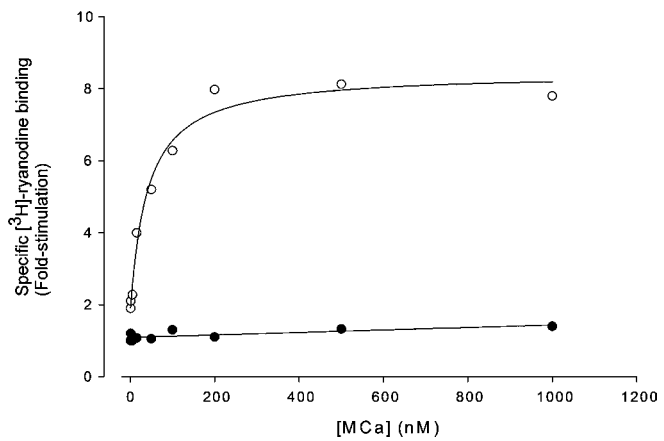

Figure 3 MCa does not modify [^{3}H]ryanodine binding on RyR2

[^{3}H]Ryanodine binding on skeletal and cardiac vesicles was measured in the presence of 5 nM [^{3}H]ryanodine and various concentrations of MCa as described in the Experimental section. Multiplication factor of [^{3}H]ryanodine binding on skeletal vesicles (○) and cardiac vesicles (●) are presented as a function of MCa concentration. Non-specific binding remained constant independently of MCa concentrations and represented less than 8 % of total binding. Each point was performed in triplicate. Data obtained with skeletal vesicles were fitted with the following equation: $y = y_0 + ax/b + x$ with a = 7.205 ± 0.564 and b = 25.58 ± 9.42.

on SR vesicles isolated from canine heart enriched in RyR2. The results presented in Figure 3 show that, while MCa induces a strong increase of [^{3}H]ryanodine binding on RyR1 (7-fold

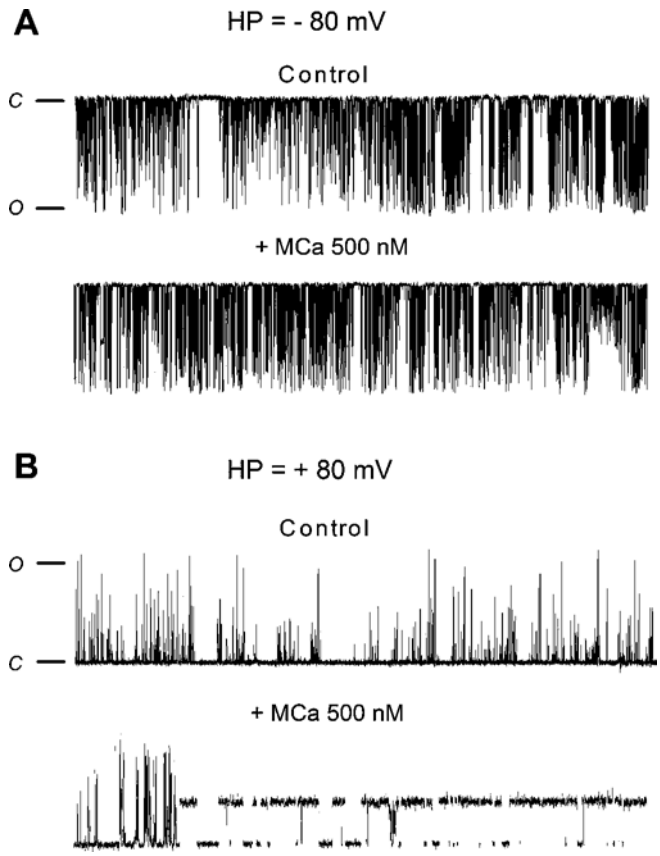

Figure 4 MCa effect on RyR2 gating properties

Representative current traces of control and MCa-induced RyR2 channel activity. Purified RyR2 was incorporated in a planar lipid bilayer and its single-channel activity recorded as described in the Experimental section. The holding potential was −80 mV in (**A**) and +80 mV in (**B**). The conductance of RyR2 was approx. 500 pS. The time duration of each record is 20 s. The closed and opened states of the channel are designated by *C* and *O* respectively. MCa was applied at a concentration of 500 nM in the *cis* chamber containing a free Ca^{2+} concentration of 472 nM.

increase of B_{max}, EC_{50} 2558 ± 9.42 nM), it promotes a very small and non-saturating (up to 2 μM) effect on [^{3}H]ryanodine binding on RyR2. Since RyR2 differs from RyR1 in its dependence on the cytoplasmic Ca^{2+} concentration, the effect of MCa on RyR2 was also tested in the presence of higher Ca^{2+} concentrations (pCa 4). No significant changes were observed for the effect of MCa on RyR2 (results not shown).

Single-channel analysis of MCa effects on RyR2 channel

We next studied the effect of MCa on the gating properties of RyR2. Purified RyR2 was incorporated into an artificial lipid bilayer and MCa was added to the *cis* chamber which corresponds to the cytoplasmic face of the RyR2 channel. We previously showed that MCa affects the RyR1 gating behaviour by inducing: (i) an increase of the opening probability (P_o), and (ii) the appearance of characteristic LLSS (long-lasting subconductance states) [8]. These LLSS correspond to the opening RyR1 at an intermediate conductance state for extremely long periods of time, up to a few seconds.

Figure 4 shows representative traces of single RyR2 channel activity before and after application of 500 nM MCa on to the cytoplasmic side of RyR2 (*cis* chamber). Current recordings were performed by imposing two ionic current directions, corresponding to (i) the physiological direction, from the RyR2

Table 1 Characterization of the MCa effect on RyR2 gating behaviour

Single-channel recording of purified RyR2 or RyR1 incorporated in an artificial lipid bilayer were performed as described in the Experimental section. Physiological current direction corresponds to ionic flux from the luminal face of the RyR to its cytoplasmic face, whereas reverse current direction corresponds to an ionic flux from the cytoplasm face of the RyR to its luminal side. n.d., not detectable.

(a) P_o

MCa concentration (nM)	RyR2 physiological current direction	RyR2 reverse current direction	RyR1 reverse current direction
0	0.034 ± 0.014	0.007 ± 0.005	0.02 ± 0.007
50	0.061 ± 0.021	0.009 ± 0.003	0.21 ± 0.016
100	0.058 ± 0.020	0.011 ± 0.007	0.24 ± 0.021
500	0.068 ± 0.023	0.010 ± 0.008	0.31 ± 0.047

(b) Number of LLSS events/min

MCa concentration (nM)	RyR2 physiological current direction	RyR2 reverse current direction	RyR1 reverse current direction
0	0	0	0
50	0	136.3 ± 53.2	19.7 ± 9.3

(c) Average LLSS duration (ms)

MCa concentration (nM)	RyR2 physiological current direction	RyR2 reverse current direction	RyR1 reverse current direction
0	n.d.	n.d.	n.d.
50	n.d.	192.7 ± 14.7	12037 ± 875
100	n.d.	186.2 ± 33.5	10236 ± 187
500	n.d.	217.7 ± 67.2	13371 ± 245

luminal side (*trans* chamber) to the cytoplasmic side, or (ii) the reverse direction, from the RyR2 cytoplasmic side to the luminal side. The results presented in Figure 4 and Table 1 show major differences in the effect of MCa on RyR2 compared with its effect on RyR1: (i) in the physiological direction of the ionic current, neither LLSS events nor significant change of P_o were observed after addition of MCa on RyR2 (Figure 3A), and (ii) in the reversed direction of the ionic current, addition of MCa induced the appearance of LLSS events on RyR2 (Figure 3B) different from those observed on RyR1. Indeed, a statistical comparison of RyR1 and RyR2 LLSS induced by MCa in the reverse direction (Table 1) shows a much shorter duration of RyR2 single LLSS (192.7 ± 14.7 ms for RyR2 compared with 12037 ± 875 ms for RyR1). In the reverse direction current condition, no significant change of P_o value (measured during inter-LLSS periods) was observed in the presence of MCa.

MCa fails to induce Ca^{2+} release from cardiac HSR vesicles

In order to investigate further a possible effect of MCa on RyR2, we studied the ability of MCa to induce Ca^{2+} release from SR vesicles purified from canine heart. Cardiac HSR vesicles were actively loaded with four consecutive additions of Ca^{2+} (20 μM) in the presence of pyrophosphate, ATP-Mg and an ATP-regenerating system, and then submitted to different concentrations of MCa. Extravesicular Ca^{2+} concentration changes were measured using Antipyrylazo III as a Ca^{2+} indicator. Figure 5(A) shows that the addition of MCa at 25 nM (final concentration) to the loaded skeletal HSR vesicles induced a strong increase in the extravesicular Ca^{2+} concentration corresponding to the release of up to 82 % of the Ca^{2+} contained in the HSR vesicles. In contrast, addition of up to 1 μM MCa (final concentration) to cardiac SR vesicles did not induce any increase in the extravesicular Ca^{2+} concentration and thus any Ca^{2+} release from the vesicles (Figure 5B). In order to assess the functional integrity of the cardiac HSR vesicles and Ca^{2+} release process through RyR2, thymol, a previously described agonist of RyR2 [19], was added to the extravesicular medium. As seen in Figure 5(B), addition of thymol (1.5 mM final concentration) induces a strong increase in extravesicular Ca^{2+} concentration corresponding to the release of 45 % of the Ca^{2+} contained in the cardiac HSR vesicles. This effect of thymol demonstrates both the tight sealing of the cardiac HSR vesicles and the functionality of RyR2. These results demonstrate that MCa is unable to induce Ca^{2+} release from cardiac HSR vesicles.

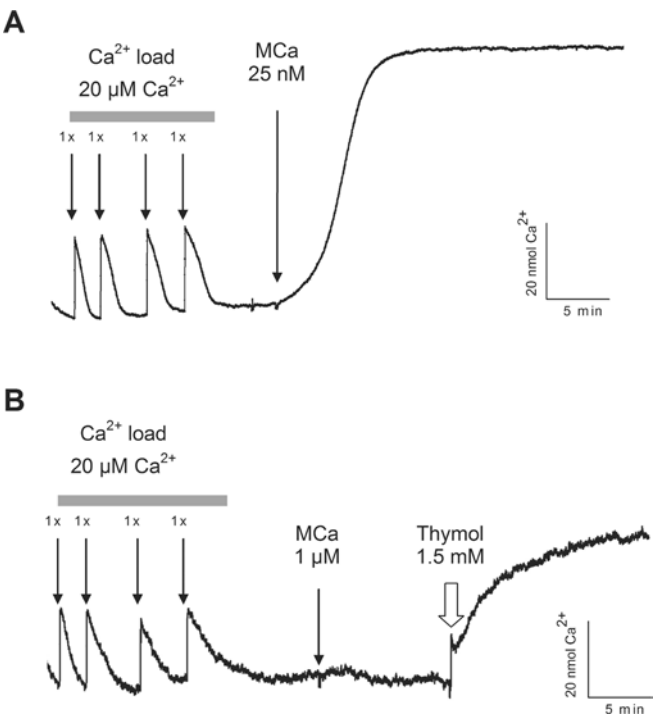

Figure 5 MCa fails to induce Ca^{2+} release from cardiac HSR vesicles

Representative traces of extravesicular Ca^{2+} concentration variations measured using Antipyrylazo III, a Ca^{2+} indicator. Skeletal HSR vesicles (**A**) and cardiac HSR vesicles (**B**) were actively loaded with Ca^{2+} by sequential addition of 20 μM $CaCl_2$ (final concentration) in the cuvette. After each Ca^{2+} addition, the absorbance was monitored until the initial baseline value was reached. MCa-induced Ca^{2+} release was then tested on skeletal and cardiac HSR vesicles by addition of 25 nM MCa to skeletal HSR (**A**) and 1 μM MCa to cardiac HSR (**B**). Integrity of the cardiac vesicles and functionality of the RyR2 channel were assessed by injection of 1.5 mM thymol, 10 min after the application of MCa.

DISCUSSION

In the present study, we evaluated the putative activation of RyR2 by MCa. We demonstrate that MCa is able to interact directly with purified RyR2. This interaction involves at least two domains homologous with those of RyR1 identified previously as MCa-binding sites. We also show that MCa does not induce any changes either in [^{3}H]ryanodine binding on RyR2 or in RyR2-channel gating properties. In support of these results, we show that MCa fails to promote Ca^{2+} release from cardiac HSR.

In previous work, we have characterized MCa as one of the most powerful effectors of RyR1 [8] and identified two discrete domains (F3 and F7) of RyR1 responsible for the binding of MCa [14]. In the present study, we show that despite the fact that MCa interacts with RyR2 on the domains homologous with F3 and F7, MCa is unable to induce the characteristic functional modifications that it promotes on RyR1. These results suggest that, whereas F3 and F7 domains are directly involved in the control of the RyR1 gating process, they exert a completely different control on RyR2 gating behaviour. Therefore MCa presents specificity for the skeletal compared with the cardiac RyR isoform in terms of functional effect, although it does not show specificity in terms of interaction. To our knowledge MCa is the first molecule shown to interact with the homologous sequences of RyR1 and RyR2, and yet presents a completely different effect on each isoform. IpTxA has been shown to modify, although to a much slighter degree than MCa, the gating properties of RyR1 [20–22] and various degrees of effect of this toxin on RyR2 have been described [23,24]. Therefore, in comparison with MCa, IpTxA shows a much weaker effect and a much less functional specificity between RyR1 and RyR2. A significant effect of MCa on RyR2 conductance was observed when the imposed current was in the opposite direction compared with the physiological situation during Ca^{2+} release (positive potential). The subconductance events induced by MCa in these conditions were however much shorter than those observed on RyR1 at both positive and negative potentials. In its primary amino acid sequence, MCa presents a cluster of basic residues. Structural data show that these residues form a positively charged surface [6]. Consequently, at positive potential, the electric field could provoke an accumulation of MCa at the vicinity of the pore region of RyR2 responsible for the conductance reducer effect observed.

The effects of MCa on RyR1 indicate that MCa strongly activates RyR1 channel opening. This effect could result from the direct implication of the MCa-binding sites (i.e. the F3 and F7 domains) in the pore-forming region of RyR1 or from the destabilization, following MCa binding, of an intramolecular 'brake' that would, through a distance effect, allow RyR1 opening. In the first hypothesis, the absence of an MCa effect on RyR2 would suggest a completely different three-dimensional topology of RyR2 channel moiety, excluding the homologous domains of F3 and F7 from the pore region. In the second hypothesis, the lack of MCa effect on RyR2 would highlight the presence on RyR2 of a different intra-molecular brake insensitive to MCa binding. Previous studies using chimaeric RyRs have shown that the functional importance of a specific domain of RyR1 differs when this domain is expressed in a RyR3 or RyR2 background, revealing that several domains of RyRs are involved in the channel-gating process [25,26]. All together these results seem to favour the second hypothesis, the difference in MCa effect on RyR1 and RyR2 being due to the lack of signal transduction from the MCa-binding domains to the pore domain in RyR2.

Interestingly, we recently demonstrated that MCa shares common binding sites on RyR1 with a domain of the cytoplasmic II-III loop of the DHPR $Ca_v1.1$ subunit [14]. Based on the effect of MCa on Ca^{2+} sparks in skeletal muscle cells and on the closure kinetics of RyR1 following the repolarization of the plasma membrane, we proposed that this domain of the DHPR could be a regulator of the RyR1 internal brake [11,12]. Therefore the absence of an effect of MCa on RyR2 could reflect a physiological difference in the role of the corresponding domain of the cardiac DHPR $Ca_v1.2$ subunit in the control of RyR2 gating behaviour.

This work was supported by grants from the European Commission (HPRN-CT-2002-00331), Association Française contre les Myopathies, Hungarian Research Foundation (OTKA T 61442) and by INSERM, CEA (Commissariat à l'Énergie Atomique) and UJF (Université Joseph Fourier).

REFERENCES

1 Fill, M. and Copello, J. A. (2002) Ryanodine receptor calcium release channels. Physiol. Rev. **82**, 893–922
2 Tanabe, T., Mikami, A., Numa, S. and Beam, K. G. (1990) Cardiac-type excitation-contraction coupling in dysgenic skeletal muscle injected with cardiac dihydropyridine receptor cDNA. Nature **344**, 451–453
3 Nakai, J., Ogura, T., Protasi, F., Franzini-Armstrong, C., Allen, P. D. and Beam, K. G. (1997) Functional nonequality of the cardiac and skeletal ryanodine receptors. Proc. Natl. Acad. Sci. U.S.A. **94**, 1019–1022
4 el-Hayek, R., Lokuta, A. J., Arevalo, C. and Valdivia, H. H. (1995) Peptide probe of ryanodine receptor function: imperatoxin A, a peptide from the venom of the scorpion *Pandinus imperator*, selectively activates skeletal-type ryanodine receptor isoforms. J. Biol. Chem. **270**, 28696–28704
5 Zhu, X., Zamudio, F. Z., Olbinski, B. A., Possani, L. D. and Valdivia, H. H. (2004) Activation of skeletal ryanodine receptors by two novel scorpion toxins from *Buthotus judaicus*. J. Biol. Chem. **279**, 26588–26596
6 Mosbah, A., Kharrat, R., Fajloun, Z., Renisio, J. G., Blanc, E., Sabatier, J. M., El Ayeb, M. and Darbon, H. (2000) A new fold in the scorpion toxin family, associated with an activity on a ryanodine-sensitive calcium channel. Proteins **40**, 436–442
7 Shahbazzadeh, D., Srairi-Abid, N., Feng, W., Ram, N., Borchani, L., Ronjat, M., Akbari, A., Pessah, I. N., De Waard, M. and El Ayeb, M. (2007) Hemicalcin, a new toxin from the Iranian scorpion *Hemiscorpius lepturus* which is active on ryanodine-sensitive Ca^{2+} channels. Biochem. J. **404**, 89–96
8 Esteve, E., Smida-Rezgui, S., Sarkozi, S., Szegedi, C., Regaya, I., Chen, L., Altafaj, X., Rochat, H., Allen, P., Pessah, I. N. et al. (2003) Critical amino acid residues determine the binding affinity and the Ca^{2+} release efficacy of maurocalcine in skeletal muscle cells. J. Biol. Chem. **278**, 37822–37831
9 Tanabe, T., Beam, K. G., Adams, B. A., Niidome, T. and Numa, S. (1990) Regions of the skeletal muscle dihydropyridine receptor critical for excitation-contraction coupling. Nature **346**, 567–569
10 Dulhunty, A. F., Curtis, S. M., Watson, S., Cengia, L. and Casarotto, M. G. (2004) Multiple actions of imperatoxin A on ryanodine receptors: interactions with the II-III loop "A" fragment. J. Biol. Chem. **279**, 11853–11862
11 Pouvreau, S., Csernoch, L., Allard, B., Sabatier, J. M., De Waard, M., Ronjat, M. and Jacquemond, V. (2006) Transient loss of voltage control of Ca^{2+} release in the presence of maurocalcine in skeletal muscle. Biophys. J. **91**, 2206–2215
12 Szappanos, H., Smida-Rezgui, S., Cseri, J., Simut, C., Sabatier, J. M., De Waard, M., Kovacs, L., Csernoch, L. and Ronjat, M. (2005) Differential effects of maurocalcine on Ca^{2+} release events and depolarization-induced Ca^{2+} release in rat skeletal muscle. J. Physiol. **565**, 843–853
13 Shtifman, A., Ward, C. W., Wang, J., Valdivia, H. H. and Schneider, M. F. (2000) Effects of imperatoxin A on local sarcoplasmic reticulum Ca^{2+} release in frog skeletal muscle. Biophys. J. **79**, 814–827
14 Altafaj, X., Cheng, W., Esteve, E., Urbani, J., Grunwald, D., Sabatier, J. M., Coronado, R., De Waard, M. and Ronjat, M. (2005) Maurocalcine and domain A of the II-III loop of the dihydropyridine receptor Cav 1.1 subunit share common binding sites on the skeletal ryanodine receptor. J. Biol. Chem. **280**, 4013–4016
15 Marty, I., Robert, M., Villaz, M., De Jongh, K., Lai, Y., Catterall, W. A. and Ronjat, M. (1994) Biochemical evidence for a complex involving dihydropyridine receptor and ryanodine receptor in triad junctions of skeletal muscle. Proc. Natl. Acad. Sci. U.S.A. **91**, 2270–2274
16 Anderson, K., Lai, F. A., Liu, Q. Y., Rousseau, E., Erickson, H. P. and Meissner, G. (1989) Structural and functional characterization of the purified cardiac ryanodine receptor-Ca^{2+} release channel complex. J. Biol. Chem. **264**, 1329–1335
16a Bradford, M. M. (1976) A rapid and sensitive method for the quantitation of microgram quantities of protein utilizing the principle of protein-dye binding. Anal. Biochem. **72**, 248–254

17 Lai, F. A., Erickson, H. P., Rousseau, E., Liu, Q. Y. and Meissner, G. (1988) Purification and reconstitution of the calcium release channel from skeletal muscle. Nature **331**, 315–319
18 Thompson, J. D., Higgins, D. G. and Gibson, T. J. (1994) CLUSTAL W: improving the sensitivity of progressive multiple sequence alignment through sequence weighting, position-specific gap penalties and weight matrix choice. Nucleic Acids Res. **22**, 4673–4680
19 Szentandrassy, N., Szigeti, G., Szegedi, C., Sarkozi, S., Magyar, J., Banyasz, T., Csernoch, L., Kovacs, L., Nanasi, P. P. and Jona, I. (2004) Effect of thymol on calcium handling in mammalian ventricular myocardium. Life Sci. **74**, 909–921
20 Valdivia, H. H., Kirby, M. S., Lederer, W. J. and Coronado, R. (1992) Scorpion toxins targeted against the sarcoplasmic reticulum Ca^{2+}-release channel of skeletal and cardiac muscle. Proc. Natl. Acad. Sci. U.S.A. **89**, 12185–12189
21 Gurrola, G. B., Arevalo, C., Sreekumar, R., Lokuta, A. J., Walker, J. W. and Valdivia, H. H. (1999) Activation of ryanodine receptors by imperatoxin A and a peptide segment of the II-III loop of the dihydropyridine receptor. J. Biol. Chem. **274**, 7879–7886
22 Zamudio, F. Z., Gurrola, G. B., Arevalo, C., Sreekumar, R., Walker, J. W., Valdivia, H. H. and Possani, L. D. (1997) Primary structure and synthesis of Imperatoxin A [IpTx(a)], a peptide activator of Ca^{2+} release channels/ryanodine receptors. FEBS Lett. **405**, 385–389
23 Tripathy, A., Resch, W., Xu, L., Valdivia, H. H. and Meissner, G. (1998) Imperatoxin A induces subconductance states in Ca^{2+} release channels (ryanodine receptors) of cardiac and skeletal muscle. J. Gen. Physiol. **111**, 679–690
24 Simeoni, I., Rossi, D., Zhu, X., Garcia, J., Valdivia, H. H. and Sorrentino, V. (2001) Imperatoxin A [IpTx(a)] from *Pandinus imperator* stimulates [^{3}H]ryanodine binding to RyR3 channels. FEBS Lett. **508**, 5–10
25 Nakai, J., Sekiguchi, N., Rando, T. A., Allen, P. D. and Beam, K. G. (1998) Two regions of the ryanodine receptor involved in coupling with L-type Ca^{2+} channels. J. Biol. Chem. **273**, 13403–13406
26 Perez, C. F., Voss, A., Pessah, I. N. and Allen, P. D. (2003) RyR1/RyR3 chimeras reveal that multiple domains of RyR1 are involved in skeletal-type E–C coupling. Biophys. J. **84**, 2655–2663

Received 2 April 2007/15 May 2007; accepted 31 May 2007
Published as BJ Immediate Publication 31 May 2007, doi:10.1042/BJ20070453